# Estimating the age of volcanism in Seamount Provinces of the Northeast Indian Ocean

**Rajat Taneja**
*Department of Earth and Planetary Sciences,*
*Core to Crust Fluid Systems ARC Centre of Excellence*
*GEMOC ARC National Key Centre,*
*Macquarie University, Sydney,*
*rajat.taneja@mq.edu.au*

**Craig O'Neill**
*Department of Earth and Planetary Sciences,*
*Core to Crust Fluid Systems ARC Centre of Excellence*
*GEMOC ARC National Key Centre,*
*Macquarie University, Sydney*
*craig.oneill@mq.edu.au*

## SUMMARY

The breakup of Australian landmass from Greater India, part of the late dispersal of Gondwana, started around 136 Ma. Concurrent with this breakup was the eruption of significant volumes of volcanics, on both the continental margins of Australia and India, including the North-West shelf, and in the ocean basin separating the two. Later submarine volcanism occurred within the Christmas Island Seamount Province (ChrISP), or which Christmas and Cocos (Keeling) Islands are two subareal examples. These volcanic events significantly impacted the thermal evolution of these margins, but the ultimate cause for this disparate volcanism, and the relationship between margin volcanics and later submarine volcanic events, remains unclear. The study tries to establish a relation between the volcanic activities and look for any evidence of these volcanic episodes. The study uses gravity, magnetic, and subsidence modelling to attempt to constrain the structure and ages of seamount volcanism within the Christmas Island Seamount Province, including the Wharton Basin and Argo Abyssal Plain. Gravity modelling helps to determine the crustal structure and constrains the depth of limestone cap, which further helps in calculating when the seamount was sub aerially exposed and approximates the time since it was last exposure. The relationship between the volcanism observed in the ChrISP (Late Cretaceous to Eocene) and that recorded earlier on the NW shelf continental margin, remains ambiguous, and will be better constrained with forthcoming geochemical analysis. But the results presented here point to a rich and complex history of volcanism within the Indo-Australian plate.

**Keywords**: Seamounts, Cocos (Keeling) Islands, Christmas Island, Paleolatitude, Gravity Modelling

## INTRODUCTION

The first sign of intercontinental rifting of Gondwana started in the Permian and Triassic and led to eventual rupturing of south-western Australia. Early Cretaceous saw the basaltic eruption of Bunbary Basalt (Western Australia) and Rajmahal Traps (Northeast India), associated with Kerguelen plume head, and the separation of India and Australia (Veevers, 1971). The presence of magnetic anomaly M25 [154.1 Ma] (Stagg *et al.* 1999; Heine and Müller, 2005) in the Argo and Gascoyne basin suggests seafloor spreading began in the Late Jurassic.

The eastern part of the Indian Ocean consists of seamounts whose origin is not well understood. Cocos (Keeling) Islands (CKI) and Christmas Island (CI) are the two seamounts in North East Indian Ocean that rise above the sea level, however, there are many seamounts in the area that are submerged. CKI is located in the Indian Ocean approximately 2,950 km north west of Perth, and consists of a circular coral atoll above a submerged volcano. CI is a limestone capped volcanic island located about 305 km south of Java. The island lies in the Wharton Basin off the western coast of Australia, and is moving northwards in to the Java Trench at around 70-80 mm/yr (Borissova, 1994). The rocks of the islands are of late Cretaceous to early Tertiary age and consist of intermediate to basic volcanics like basalts, andesites, and trachybasalts (Grimes, 2001). The bathymetry of the North-east Indian Ocean (Figure 1) demonstrates the existence of numerous flat-topped seamounts, or guyots. One such features is shown in the profiles in Figure 2. These features are generally thought to have weathered sub-areally, to acquire their morphology, suggesting that the seamount was once above sea-level and have been subjected to erosion and weathering processes.

## METHODOLOGY AND RESULTS

This study utilises numerous geophysical approaches to constraining the age and history of the Christmas Island seamount province – including both CKI and CI. Gravity data has been used to model the thickness of limestone cover on CKI, which, together with coral deposition rates, can constrain the age of the islands. The depth below sea-level to submerged seamounts, together with a subsidence age-depth relation (Tucholke and Smoot, 1990), can be used to determine when the seamount was exposed above sea-level. Regional bathymetry data for the oceans have been employed to prepare profiles showing flat tops seamounts (Figure 2).

The ages obtained by these techniques were imported in Gplates to understand their movement over a global time scale. Gplates reconstructions are complemented with paleolatitudional calculations of drilled cores from CI in order to understand their evolution and movement on a global time scale.

**Gravity Modelling**: Gravity data was modelled for the CKI to determine the crustal structure of the oceanic realms and estimate the depth of limestone cover over the island. The regional gravity and bathymetry data sets were obtained from Scripps Institute of Oceanography, University of California. These are 1 minute grids and used in GMT to prepare gravity anomaly maps for the islands (Smith and Sandwell, 1997). The gravity data was modelled using gravity and magnetic modelling tool Modelvision version 8 by Encom. The data set in xyz format, consisting of distance (m) in X and Y coordinates and gravity anomaly values (gu), is imported in to the software to produce an observed gravity profile of the region. The ocean floor is then modelled to produce a calculated gravity profile that matches up with the observed profile. While modelling the ocean floor it was ensured that the modelled crust matches with the bathymetry of the ocean floor. During modelling, a three layer crustal structure of the ocean floor has been assumed consisting of basalt, gabbro, and mantle. Watts, *et al*. (1985) computed gravity anomalies for the Hawaiian-Emperor seamount chain and proposed two models for deep crustal structure, one with thin oceanic crust under the ridge, and other with a normal oceanic crust.

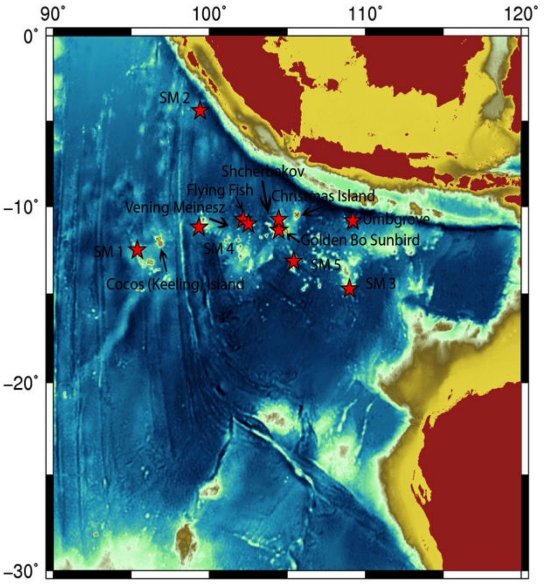


Figure 1: Map of the Northeast Indian Ocean displaying seamounts.

They have shown that the total crustal thickness is around 6.5 km beneath the Hawaiian arch and varies between 10.5 – 12.0 beneath the moat and 18.0 km under the ridge.
Similar crustal structure has been employed to our gravity analysis for CKI. The top layer of the islands consists of Pleistocene limestone. The depth of this layer is not known, however there are estimates for its depth based on dredging (IFM GEOMAR, 2009). The second layer beneath limestone is basalt. Its thickness has been assumed to be around 1.5 km according to Watts, *et al.* (1975) model. Basalts are underlain by gabbros, with thickness around 5 km. To compensate for the high gravity anomaly of the CKI, there has to be mass within the oceanic crust to balance the excess mass of the

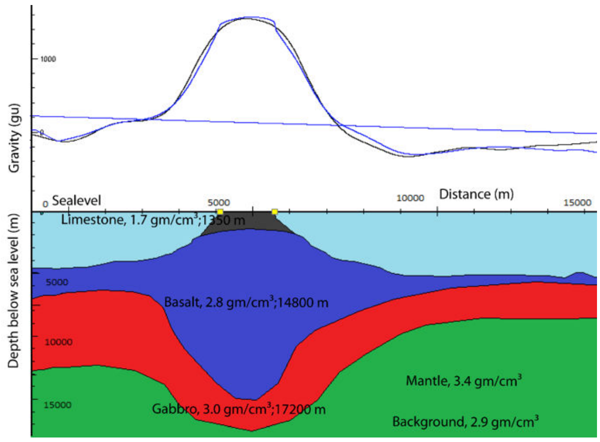


Figure 3: Gravity Modelling for Cocos (Keeling) Island at latitude 12.18°S, x-axis distance in m; positive y axis, gravity units; negative y axis depth below sea level.

island above the ocean floor. This excess mass brings the crustal structure to deeper depths, the basaltic layers extends up to 15 km whereas the gabbro reaches up to 17 km depending on the density for these layers (Figure 3). The gravity modelling for CKI is presented in Figure 3. The depth of limestone is around 1,350 m when the density of the top layer is 1.7 gm/cubic cm and it becomes 1,500 m when the density is increased to 1.85 gm/cubic cm. If we assume fixed densities for limestone, gabbro and mantle (Table 1), but change the densities of basalt, we observe that the depth of limestone cover increases (Figure 4).
Woodroff et al. (1991) calculates coral growth rate of 0.08mm/yr to 0.1 mm/yr for the atoll, and our work constrains the thickness range to be between 800m and 1500m. This gives us age estimates of about 8 to 10 Myr for a growth rate of 0.08mm/yr; and between and 15 to 18 Myr for a growth rate of 0.1 mm/yr.

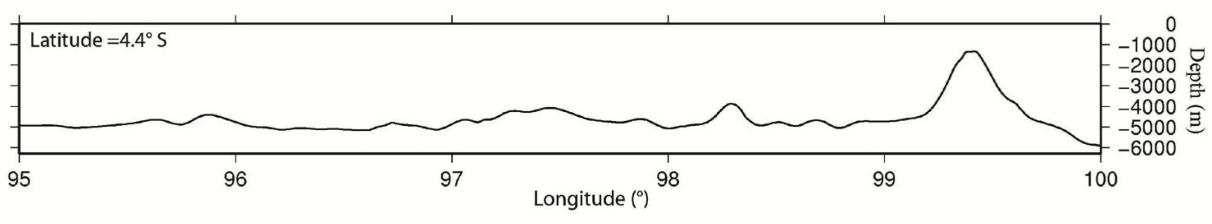


Figure 2: Profile of flat top of seamount, SM 2.

| | Density ($g/cm^3$) | Depth to base (m) | Density ($g/cm^3$) | Depth to base (m) | Density ($g/cm^3$) | Depth to base (m) | Density ($g/cm^3$) | Depth to base (m) |
|---|---|---|---|---|---|---|---|---|
| Limestone | 1.8 | 900 | 1.8 | 1100 | 1.8 | 1307 | 1.8 | 1800 |
| Basalt | 2.8 | 13700 | 2.85 | 14500 | 2.9 | 16400 | 2.95 | 17500 |
| Gabbro | 3.1 | 16000 | 3.1 | 16600 | 3.1 | 18500 | 3.1 | 19050 |
| Mantle | 3.3 | | 3.3 | | 3.3 | | 3.3 | |
| Background | 2.88 | | 2.88 | | 2.88 | | 2.88 | |

Table 1: Change in limestone thickness and crustal structure thickness with changing basaltic densities.

| Name of the Seamount | Latitude(S) | Longitude | Depth below sea level (m) | Seamount Age, Ma (using the average age of crust as 94.4) | Seamount Age, Ma (Sea floor age, using GPlates age database) |
|---|---|---|---|---|---|
| SM 1 | 12.50 | 95.40 | 1537-1635 | 66.0-68.9 | 27.5-30.4 (55.9) |
| SM 2 | 4.40 | 99.42 | 1325- 1700 | 59.2-70.8 | 20.9-32.30 (55.9) |
| SM 4 | 11.20 | 99.34 | 1156-1470 | 53.1-63.9 | 42.4-53.1 (83.5) |
| SM 5 | 13.50 | 108.73 | 2182-2400 | 82.3-86.2 | 92.9-96.8 (105) |
| SM 3 | 14.75 | 108.99 | 3126-3300 | 93.7-94.3 | 126.0-126.6 (126.7) |
| Flying Fish | 10.75 | 102.18 | 3057-3433 | 93.4-94.3 | 82.5-83.4 (83.5) |
| Golden Bo'sunbird | 11.38 | 104.46 | 294-552 | 15.6-28.1 | 26.2-38.7 (105) |
| Umbgrove | 10.83 | 109.20 | 2334-2924 | 85.1-92.5 | 95.7-103.1(105) |
| Shcherbakov | 10.75 | 104.83 | 1878-2242 | 75.4-83.4 | 80.0-89.0 (99) |
| Vening Meinesz | 11.00 | 102.40 | 2065-2844 | 79.8-91.8 | 84.4-96.4 (99) |

Table 2: Age Depth relation for flat topped peaks in East Indian Ocean.

Woodroffe *et al.* (1991) acknowledges that this growth rate is significantly faster than the rate predicted through thermal lithospheric models of that area, which is 0.0149 mm/yr (Marty and Cazenave, 1989) which would give an age in the range of 53 to 100 Myr.

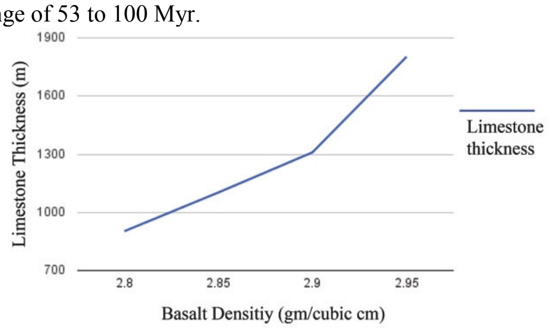


Figure 4: Increase in limestone cover thickness with increasing basaltic density.

**Age Depth Relation**: As the lithosphere moves away from the mid-oceanic ridge, it cools and begins to contract. The subsidence of the ocean floor is proportional to the square root of the age, however for larger ages it becomes exponential. This age-depth relations were further modified by Parsons and Sclater (1977) and they showed a break in the relation between 60 and 80 Ma ago., developing a 'plate' model to explain the behaviour of sea-floor of ages greater than 80Myr. Using this age-depth relation, we calculated the age when the seamount was sub aerially exposed and approximate their time of origin by back-tracking the feature from their present depth. The flat topped seamounts are evidence of the fact that they were subjected to erosion and weathering while they were exposed above the surface of the sea. We have used Parsons and Sclater (1977) and Tucholke and Smoot (1990) age-depth relation curve for the Atlantic Ocean with slight modification and used it on the Indian Ocean.

Modifying this relation for seamount subsidence in the North-East Indian Ocean we get,

$$(5900 - d_{sm})=2500 + 350*t^{1/2},$$

$$\text{or,}\quad t = \{((5900-d_{sm})-2500)/350\}^2$$

Where; 5900 is the depth of the seafloor in the region, $d_{sm}$ is the depth of the seamount, and t the age in Myr.

The age obtained from the above relation is subtracted from the age of the ocean crust, to get age the seamount was sub aerially exposed, which approximates - roughly - the age of the seamount. We did this in two ways, in the first example; we subtracted an average age of the crust which is depicted in column five in Table 2. Alternatively, we also extracted ages of the crust from the Gplates seafloor age database, to obtain seafloor ages for where that particular seamount lies, and this is depicted in column six. For this relation it is assumed that there is no other process acting to uplift or thermally reset the crust by any phase of volcanic activity (Tucholke and Smoot, 1990).

The ages obtained suggest around two stages of volcanic activity occurred in the region. The earliest was Early to Late Cretaceous; second one was Late Palaeocene to Early Eocene. This conforms with the dating of the volcanic activity on Christmas Island (Grimes, 2001), which suggested volcanic episodes in the Late Cretaceous, Early Eocene, and with the most recent one in Pliocene (Grimes, 2001).

**Paleo- Latitude determination**: Drilling was done on CI with the aim to determine the paleolatitudes of lava flows at the time of their formation. Four sites were selected for this purpose and on an average four to five samples were collected from each site. With the assistance of CSIRO, North Ryde, inclination and declination for each of the sample were determined by alternating-field demagnetisation..

Inclination, I of a sample can be used to calculate the paleolatitude by a simple relation,

$$\tan I = 2 \tan\lambda$$

where, $\lambda$, is the latitude of the paleosite.

Calculation of paleolatitudes from four samples at Christmas Islands gives us a mean latitude of -52°. However, using Gplates, we get a most southerly paleolatitude of -34°S for Christmas Islands at ~65 Myr (Figure 5). The discrepancy between latitudes is not yet reconciled.

**Plate Tectonic Reconstruction**: Seamounts picked from bathymetric plots were plotted in plate reconstruction software GPlates (Figure 5), that helps in visualizing the motion of these features in geological time from their past to present position on a global reference frame. In this the seamounts with their present positions are reconstructed using a global rotation file, containing information about different plates and their evolution with time (Gplates rotation database). Each seamount is simply assigned an age of the plate it occupies. The reconstructed image of the Christmas Island seamount province, with respect to the (fixed) global tomography model of Becker and Boschi (2002) is shown in Figure 5.

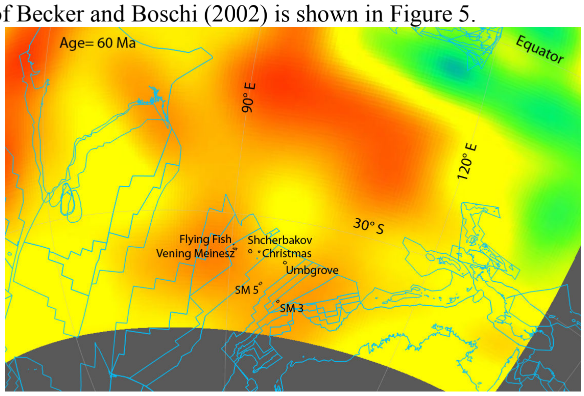


Figure 5: GPlates, plates tectonic reconstruction software, depicting paleo positions of seamounts at 60 Myr, overlying seismic tomography layer for present time (tomography model from Becker and Boschi, 2002, depth 450 km).

A distinct low velocity zone, centred around 37°S, is present in the Becker and Boschii (2002) model, which underlies the reconstructed position of the ChrISP. The low velocity anomaly is particularly prominent at the lower latitudes around the present positions these seamounts, suggesting a mantle contribution to their origin.

**Conclusion:**

The seamount province of the Northeast Indian Ocean indeed present a very rich and complex evolutionary history. The source for this volcanism is still presently not clear. Seismic tomography data analysed by Montelli *et al.* (2004) reveal the presence of an East Indian Ocean mantle plume, extending from the sublithosphere to 1900 km, with a radius of 400 km (Figure 5). We believe that this shallow mantle plume may power the seamount system in the Northeast Indian Ocean.
Gravity modelling for these islands helps us in understanding the crustal structure of the island and determines the depth of limestone. Our estimate of limestone depth for CKI of 800 to 1500m matches well with the depth ranges suggested by IFM-GEOMAR 2009. Using our age-depth techniques, stated above, we infer that the basalts were exposed around 19 Myr ago. This matches well with the subsidence age (15-19 Myr) obtained by coral accretion rates of 0.08 mm/yr by Woodroffe et al. (1991). We identified four flat top seamounts from the bathymetry data of the area, indicating they were once above sea-level and were subjected to erosion and weathering. Two of those have shallow depths in the range of 1300 to 1600m implying that they were above the surface in Early Oligocene to Early Miocene (32.3-20.9 Ma) for SM 2 and Early to Late Oligocene (30.4-27.5 Ma) for SM 1. SM 4 has an age of 53-42 Ma (Early to Middle Eocene) and SM 5 was exposed above sea-level during Late Cretaceous (93-97 Ma). This is concurrent with the earliest volcanic episodes (Late Cretaceous) on Christmas Island; subsequent events were dated as Eocene (35-40 Ma) and the most recent in Pliocene (3-5 Ma) by Grimes, 2001. Recent work by Hoernle *et al.* 2011 on Ar/Ar has shown a decreasing age trend from Agro Basin (136 Ma) in east to CKI (56-47 Ma) in the west, however, CI offsets this trend with ages of 44-4 Ma.

**References:**

Becker, T. W. and Boschi, L., 2002, A comparison of tomographic and geodynamic mantle models: Geochemistry, Geophysics, Geosystems, 3, 2001GC000168.
Borissova, I., 1994, Seafloor morphology and tectonics of the Christmas Island area, Indian Ocean: Australian Geological Survey Organisation, 1994/2.
Crawford, A. R., 1969, India, Ceylon and Pakistan: New Age Data and Comparisons with Australia: Nature 223, 380-384.
IFM-GEOMAR., 2009, Christmas Island seamount province and the Investigator Ridge: Age and causes of intraplate volcanism and geodynamic evolution of the south-eastern Indian Ocean: Liebniz Institute for Marine Sciences RV Sonne Cruise Report, SO199 CHRISP, Indonesia-Singapore: 2 August – 22 September 2008, 210 pp.
Grimes, K. G.,2001, Karst Features of Christmas Islands: Helictite 37, 41-58.
Heine, C. and Müller, R.D., 2005, Late Jurassic rifting along the Australian North West Shelf: margin geometry and spreading ridge configuration: Australian Journal of Earth Sciences: An International Geoscience Journal of the Geological Society of Australia, 52(1), 27 - 39.
Hoernle, K., Hauff, F., Werner, R., van den. Bogaard, P., Conrad, S., Gibbons, A., and Müller, D., 2011, The Christmas Island Seamount Province, Indian Ocean: Origin of intraplate volcanism by shallow recycling of continental lithosphere?: Goldschmidt 2011,Prague, Abstract,1032.
Marty, J. C. and Cazenave, A., 1989, Regional variations in subsidence rate of oceanic plates: a global analysis: Earth and Planetary Science Letters, 94(3-4), 301-315.
McElhinny, M.W. and Evans,M.E., 1968, An investigation of the strength of the geomagnetic field in the early precambrian: Physics of The Earth and Planetary Interiors 1(7), 485-497.
Montelli, R., Nolet, G., Dahlen, F. A., Masters, G., Engdahl, E., Robert Hung, Shu-Huei, 2004, Finite-Frequency Tomography Reveals a Variety of Plumes in the Mantle: Science, 303(5656), 338-343.
Parsons, B. and Sclater, J.G., 1977, An Analysis Of The Variation Of Ocean Floor Bathymetry And Heat Flow With Age: Journal of Geophysical Research, 82(5), 803-827.
Sandwell, D. T. and Smith, W.H. F., 1997, Marine gravity anomaly from Geosat and ERS 1 satellite altimetry: Journal of Geophysical Research, 102, 10039-10054.
Stagg, H. M. J., Wilcox, J.B., Symonds, P.A., O'Brein, G.W., Colwell, J.B., Hill P. J. A., Lee C-S., Moore A. M. G., Struckmeyer, I. M., 1999, Architecture and evolution of the Australian continental margin: AGSO Journal of Australian Geology & Geophysics, 17, 17 - 33.
Trueman, N. A.,1965, The phosphate, volcanic and carbonate rocks of Christmas Island (Indian Ocean): Journal of the Geological Society of Australia, 12(2), 261 - 283.
Tucholke, B. E. and Smoot, N.C., 1990, Evidence for Age and Evolution of Corner Seamounts and Great Meteor Seamount Chain From Multibeam Bathymetry: Journal of Geophysical Research, 95(B11), 17555-17569.
Veevers, J. J., 1971. Phanerozoic history of Western Australia related to continental drift: Journal of the Geological Society of Australia, 18(2), 87-96.
Watts, A. B., Cochran, J. R., Selzer, G., 1975, Gravity Anomalies and Flexure of the Lithosphere: A Three-Dimensional Study of the Great Meteor Seamount, Northeast Atlantic: Journal of Geophysical Research, 80, 1391-1398.
Watts, A. B., ten Brink, U.S., Buhl, P., Brocher, T.M., 1985, A multichannel seismic study of lithospheric flexure across the Hawaiian-Emperor seamount chain: Nature, 315, 105-111.
Woodroffe, C. D., Veeh, H. H., Falkland, A., McLean, R.F., Wallensky,E., 1991 Last interglacial reef and subsidence of the Cocos (Keeling) Islands, Indian Ocean: Marine Geology, 96, 137- 143